Kinetic C−H Oxidative Addition vs Thermodynamic C−X Oxidative Addition of Chlorobenzene by a Neutral Rh(I) System. A Density Functional Theory Study†

Hong Wu and Michael B. Hall*

Department of Chemistry, Texas A&M University, College Station, Texas 77843-3255

Received: March 29, 2009; Revised Manuscript Received: August 28, 2009

Density functional theory (DFT) is used to explore competitive C−H and C−Cl oxidative additions (OA) of chlorobenzene by the neutral Rh(I) complex: (PNP)Rh^I [PNP = bis(*Z*-2-(dimethylphosphino)vinyl)amino]. Consistent with experimental results, our calculation shows that C−Cl OA ($\Delta G^{\ddagger}$ = 16.0 kcal·mol^{-1}) is kinetically competitive with C−H OA ($\Delta G^{\ddagger}$ = 16.7 kcal·mol^{-1}) and that the C−Cl OA is thermodynamically preferred by 28.3 kcal·mol^{-1} over the most stable C−H OA product. Hence, the only experimentally observed product was from C−Cl OA.

Introduction

Carbon−hydrogen bond activation by transition metal complexes, an extremely important process in functionlizing hydrocarbons, has been studied extensively by both experimental and theoretical investigations[1] since the pioneering studies of methane activation by Shilov,[2] Bergman,[3] Jones,[4] and Graham.[5] The group 9 metals[6] have played a central role in the expansion of this challenging field; their complexes, especially those of iridium,[7] have been intensively investigated in C−H activation.

The ability to selectively and catalytically activate C−H bonds has tremendous utility in organic synthesis. Because of their strength, C−X bonds in haloarenes, commonly used organic substrates,[8] are expected to be less likely to undergo oxidative additions to transition metal species than the C−H bonds. However, the C−X bond polarity can increase the binding tendency of the C−X bonds over that of the C−H bonds, so a given metal−ligand complex may prefer to activate one of these bonds over the other. Due to steric effects, C−H bond activation in haloarenes usually takes place at the less hindered positions, forming predominantly in a mixture of meta- and para-activated complexes. However, Milstein and co-workers recently described an unprecedented ortho C−H activation preference (at ≤60 °C) in chloro- and bromobenzene via oxidative addition to the cationic [(PNP*)Ir^I]$^+$ [PNP* = 2,6-bis((di-*tert*-butylphosphino)methyl)pyridine] where the halogen acts as a directing group (I in Scheme 1).[9] It is now well established that this highly electron-donating and bulky tridentate PNP ligand generates unusual transition-metal chemistry.[10] No C−X activation products were observed in this study. More recently, Ozerov and co-workers reported a similar ortho activation preference for C−H oxidative addition, but importantly, this preference was kinetic at 70 °C, and the thermodynamic preference was for C−X (X = Cl, Br) addition at >100 °C to (PNP)$Ir(H)_2$ [PNP = bis(2-(diisopropylphosphino)-4-methylphenyl)amino] (II in Scheme 1).[11] Ozerov and co-workers also recently reported that an analogous rhodium fragment (PNP)Rh^I reacts with haloarenes to produce exclusively C−X (X = Cl, Br, I) OA products in <24 h at 22 °C (III in Scheme 1).[12] These three studies all suggest that the OA reactions proceed via a 14-electron three-coordinated intermediate, [(PNP*)Ir^I]$^+$, (PNP)Ir^I, and (PNP)Rh^I, respectively.

Although there have been extensive theoretical studies of C−H bond addition in group 9 metals, there has been only one recent report in a simple $Ir(PH_3)_2(H)$ model compound of the thermodynamic vs kinetic preference of C−X bonds vs C−H bonds, respectively.[13] We have been studying the kinetic and thermodynamic behaviors of aromatic OA reactions for cationic and neutral group 9 systems; here, we report our work on the haloarene OA reactions of Rh^I to explain the experimental observations[12] (III in Scheme 1) and discuss the similarities and differences between the current neutral Rh^I complex and the cationic and neutral Ir^I complexes.

Computational Details

All geometry optimizations and frequency determinations were carried out with the Gaussian 03 package of programs[14] at the B3LYP computational level.[15] Transition states were located with the use of synchronous transit-guided quasi-Newton method.[16] The basis set used for Rh is the extended valence double-ζ LANL2DZ[17] basis set, in which 5s and 5p functions were replaced by the reoptimized functions of Couty and Hall,[18] and a set of diffuse f functions (exponent = 1.350 (Rh)) was added.[19] The LANL2DZdp basis sets were employed for phosphorus and chlorine.[20] The 6-31G(d′) basis sets were applied to all carbon, nitrogen and hydrogen atoms.[21] Our computational models have methyl groups attached to the phosphorus atoms (i.e., $P(CH_3)_2$), a compromise between the use of hydrogen atoms and the alkyl groups actually employed in the experiment (^{i}Pr).

All computed structural data are documented in the Supporting Information, and we show models only of the most relevant conformations of the reactants and products and of the transition state structure between them (Figures 1−6). Total energies *E* (in atomic units), vibrational zero-point energies VZPE (kcal·mol^{-1}), thermal energies TE (kcal·mol^{-1}, 298.15 K), and entropies *S* (cal·mol^{-1}·K^{-1}) are reported as part of the Supporting Information (Table S1). We report and discuss ΔE, ΔE_0, ΔH, and ΔG data unless noted otherwise (Table 1).

Throughout this paper, bond lengths are given in Ångstroms, bond angles in degrees, and relative reaction energies in kcal·mol^{-1}.

† Part of the "Walter Thiel Festschrift".

* Corresponding author. E-mail: mbh@mail.chem.tamu.edu.

10.1021/jp902826w CCC: $40.75
Published on Web 10/01/2009

SCHEME 1

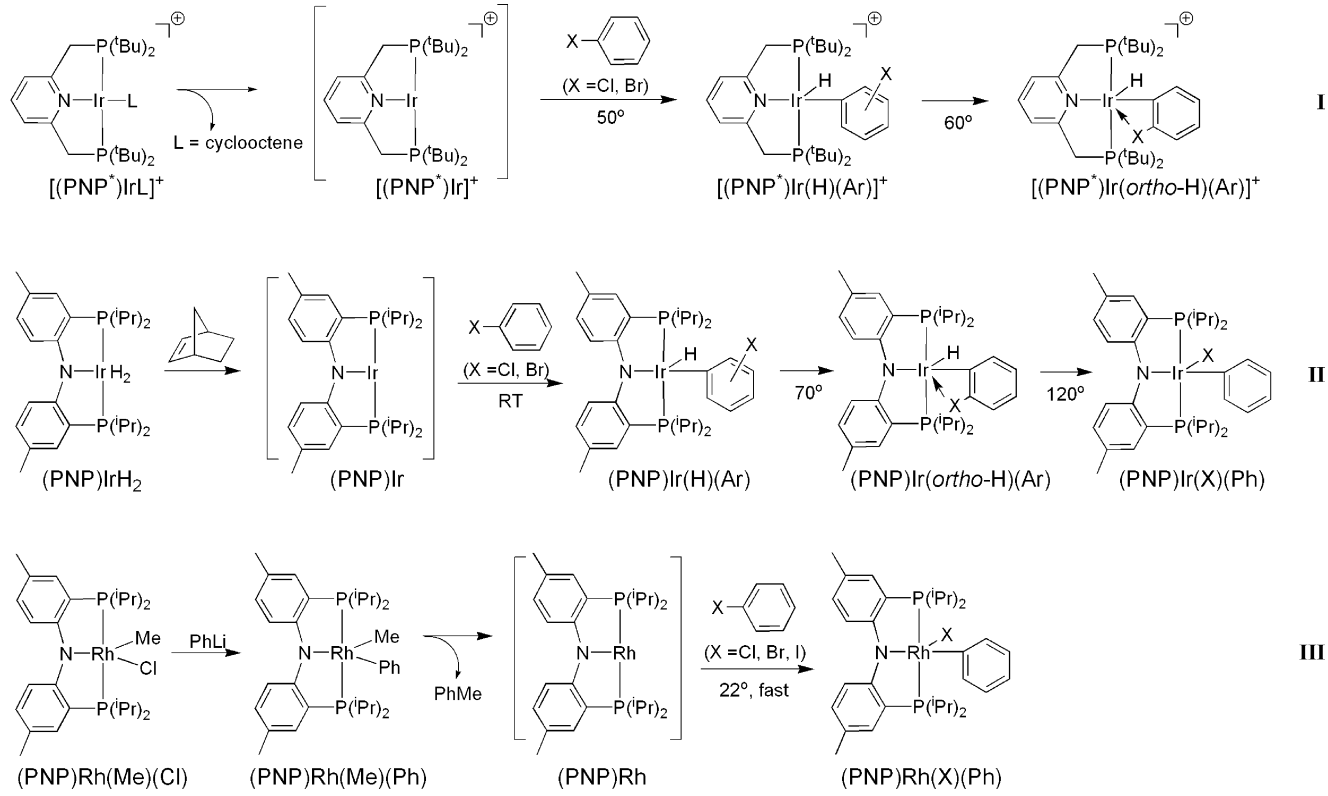

Results and Discussion

As reported, the rhodium fragment (PNP)Rh^{I} reacts with haloarenes to produce *exclusively* C−X (X = Cl, Br, I) OA products in <24 h at 22 °C (III in Scheme 1).[12] The (PNP)Rh^{I} fragment was produced via a C−C reductive elimination (RE) reaction from the complex (PNP)Rh^{I}(Ph)(Me). The kinetic study suggests that the C−C RE follows clean first-order kinetics and is the rate-determining step as the (PNP)Rh^{I} fragment rapidly undergoes C−X oxidative addition. No C−H OA products were observed. In this present study, we explore the C−C RE of **1**−**3** and both C−H and C−X OAs of **3** to **5** and **6**, repsectively (Scheme 2).

Rate-Determining C−C Reductive Elimination of 1 to 3. **1** is a five-coordinated d^6 complex, with a geometry closer to a square based pyramid than a trigonal bipyramid. Two isomers of **1** are possible depending on which group, Me or Ph, occupies the apical site (Me apical in **1a** and Ph apical in **1b**, Figure 1). **1a** is more stable than **1b** by 3.0 kcal·mol^{-1} (Table 1) and is therefore taken as the reactant for the following study.

Reductive elimination (RE) from **1** proceeds initially to an intermediate adduct between the (PNP)Rh^{I} fragment (**3**) and PhMe (**2**), **IM1**, before PhMe is lost to form **3**. Although reductive elimination leading to a carbon−carbon bond is an important step in organometallic reactions, details of the C−C RE reaction remain largely unexplored for group 9 metals. Although the transition state **TS1** resembles a C−C σ-complex (agostic) with a long C−C bond, the most stable adduct **IM1** is a Me bound η^2−H-C σ-complex (other higher energy σ- and π-complexes are also possible). The optimized geometries of **TS1** and **IM1** are shown in Figure 2. The C−C RE reaction of **1a** to **2** and **3** is exothermic (ΔH = −3.6 kcal·mol^{-1}) and exergonic (ΔG = −16.4 kcal·mol^{-1}); however, the process requires 23.3 kcal·mol^{-1} for the free-energy barrier. This relatively high barrier is in agreement with the experimental observation that the C−C RE reaction is the rate-limiting step of the entire process.

C−H and C−Cl Oxidative Addition Products. Although the C−Cl OA product is observed exclusively, we have examined both C−H and C−Cl OA reactions in this study so that we could understand why C−H OA products are not observed. Possible products from OA of chlorobenzene, **4**, to

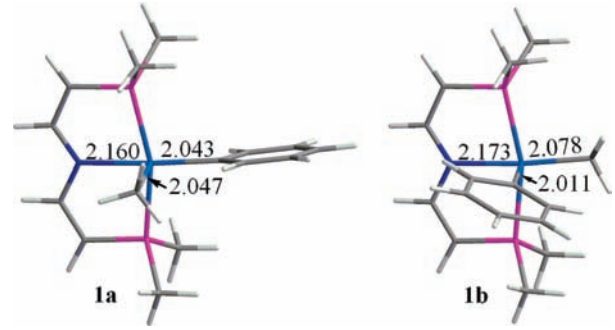

Figure 1. Optimized geometries of **1a** and **1b**.

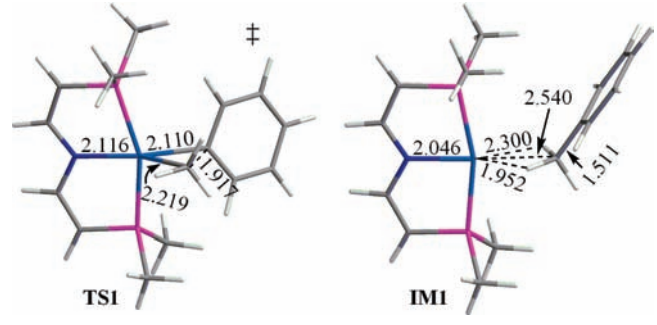

Figure 2. Optimized geometries of adduct **IM1** and transition state **TS1**.

TABLE 1: Pertinent Energies, Enthalpies, and Gibbs Free Energies (kcal·mol^{-1})

parameter		ΔE	ΔE_0	ΔH	ΔG
relative energy vs **1a**	**1b**	2.35	2.10	2.06	2.95
	IM1	−9.54	−8.44	−8.56	−9.12
relative energy vs **6**	**5a**	30.69	28.16	28.08	28.28
	5b	35.59	32.83	32.84	32.25
	5c	36.62	33.75	33.82	32.75
	5d	36.68	33.85	33.89	32.66
	5e	37.57	34.64	34.75	33.34
	7a	29.54	29.10	28.93	29.25
	7b	29.72	29.31	29.13	29.51
	7c	33.58	33.19	32.99	33.42
	IM2-a	38.33	37.45	37.58	36.14
	IM2-b	38.41	37.32	37.49	35.93
	IM2-c	37.25	36.49	36.51	35.40
	IM2-d	37.15	36.34	36.41	35.11
	IM2-e	37.07	36.32	36.35	35.31
	IM3	35.02	34.41	34.61	32.56
activation barriers	**1a → TS1**	22.60	22.69	22.19	23.28
	5a → TS(5a,5b)	17.58	17.92	17.32	19.50
	5b → TS(5a,5b)	12.68	13.25	12.56	15.53
	5c → TS(5c,5d)	3.69	4.04	3.34	6.40
	5d → TS(5c,5d)	3.63	3.94	3.27	6.48
	7a → TS2-a	19.13	16.51	16.35	16.71
	5a → TS2-a	17.99	17.45	17.19	17.68
	7a → TS2-b	15.98	13.32	13.15	13.66
	5b → TS2-b	9.94	9.59	9.24	10.65
	7a → TS2-c	14.23	11.57	11.41	11.60
	5c → TS2-c	7.16	6.91	6.52	8.11
	7a → TS2-d	14.28	11.56	11.45	11.42
	5d → TS2-d	7.14	6.81	6.49	8.01
	7b → TS2-e	14.70	11.95	11.83	11.86
	5e → TS2-e	6.85	6.62	6.21	8.04
	7a → TS3	16.56	15.99	15.86	16.03
	6 → TS3	46.10	45.08	44.79	45.28
reaction energies	**1a → 2 + 3**	−3.75	−3.25	−3.55	−16.43
	1a → IM1	−9.54	−8.44	−8.56	−9.12
	IM1 → 2 + 3	5.79	5.19	5.01	−7.31
	3 + 4 → 7a	−17.44	−16.76	−16.55	−3.88
	3 + 4 → 7b	−17.26	−16.55	−16.36	−3.62
	3 + 4 → IM2-a	−12.80	−12.43	−11.67	4.44
	3 + 4 → IM2-b	−12.82	−12.61	−11.81	4.13
	3 + 4 → IM2-c	−14.38	−13.84	−13.26	3.36
	3 + 4 → IM2-d	−14.53	−14.06	−13.41	2.92
	3 + 4 → IM2-e	−3.79	−6.79	−6.68	12.18
	3 + 4 → IM3	−11.97	−11.44	−10.87	−0.57
	7a → 5a	1.14	−0.93	−0.84	−0.97
	7a → 5b	6.04	3.73	3.91	3.01
	7a → 5c	7.07	4.65	4.89	3.50
	7a → 5d	7.14	4.75	4.96	3.41
	7b → 5e	7.85	5.34	5.62	3.82
	IM2-a → 5a	−7.64	−9.28	−9.50	−7.86
	IM2-b → 5b	−2.73	−4.49	−4.65	−3.67
	IM2-c → 5c	−0.63	−2.74	−2.69	−2.66
	IM2-d → 5d	−0.47	−2.49	−2.52	−2.45
	IM2-e → 5e	−6.85	−6.62	−6.21	−8.04
	7a → 6	−29.54	−29.10	−28.93	−29.25
	IM3 → 6	−35.02	−34.41	−34.61	−32.56

the unsaturated 14-electron (PNP)Rh^{I} complex **3** include 16-electron five-coordinate Rh^{III} complexes from both C−H OA, (PNP)Rh(H)(C_6H_4Cl) (**5**), and C−Cl OA, (PNP)Rh(Cl)(C_6H_5) (**6**) (Scheme 2).

Five isomers of C−H OA product **5** are possible, **5a**−**5e** (Figure 3), with **5a** being the lowest energy C−H OA isomer because of an additional Ph−Cl---Rh coordination. We also studied the rotation about the Rh−C for the rotamer pairs: **5a/5b**, and **5c/5d**. The rotation about Rh−C bond is relatively restricted between rotamers **5a** and **5b** ($\Delta G^{\ddagger} = 15.5$ kcal·mol^{-1}), but somewhat unrestricted between rotamers **5c** and **5d** ($\Delta G^{\ddagger} = 6.4$ kcal·mol^{-1}). The C−Cl OA product, **6**, is the thermodynamically most stable product, 28.3 kcal·mol^{-1} and 33.3 kcal·mol^{-1} lower in energy than **5a** and **5e**, respectively (Table 1). The potential isomer of **6**, which has Cl occupying the apical position, does not exist on the potential energy surface. Optimized geometries of **5a**−**5e**, **TS(5a,5b)**, **TS(5c,5d)**, and **6** are shown in Figure 3.

***η*^{2}-Coordination Products, (PNP)Rh(*η*^{2}-C_6H_5Cl), 7.** Since η^2 coordination of arenes to transition metals may occur in a step prior to oxidative addition.[22] We examined three possible isomers of the η^2-C_6H_5Cl adducts with the C−C double bond

SCHEME 2

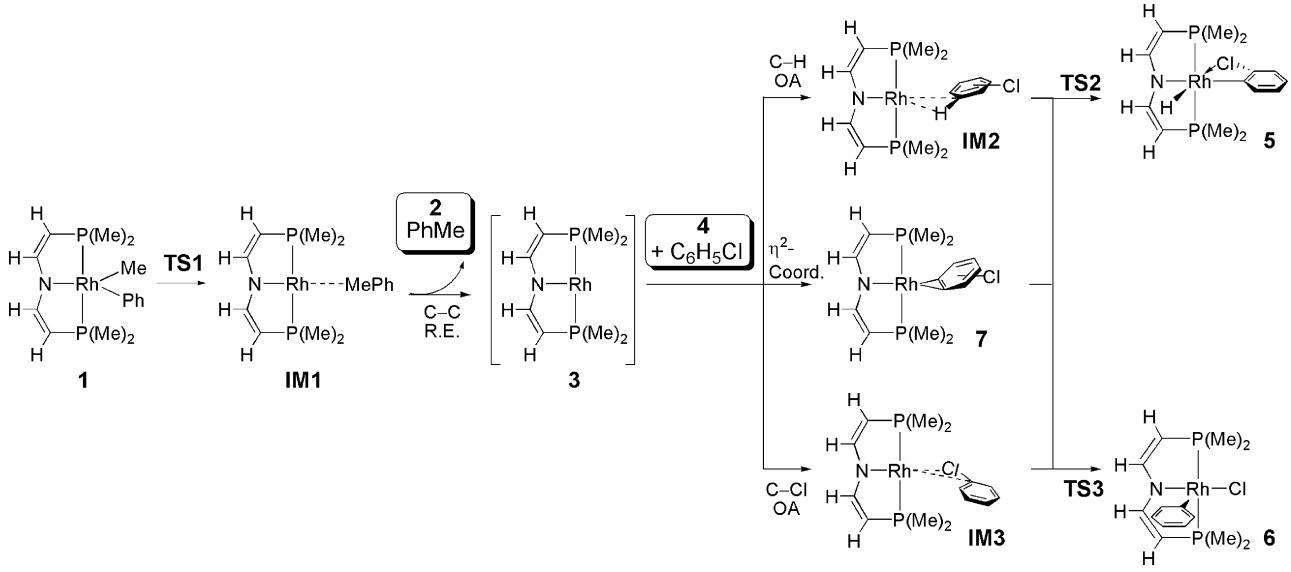

perpendicular to the pyridine plane (Figure 4). When chlorobenzene binds in an η^2 manner, the 2,3-position (site **a**) is the preferred site for η^2-coordination to **3** because the double bond character is higher between C(2) and C(3) (high population in π and low population in π^*) as a result of conjugation with the π-donor Cl. The Cl-substituted double bond (site **c**) is the least favored site by 4.2 kcal·mol^{-1} due to the decreased olefinic character at the C═C bonds adjacent to Cl. Coordination to the 3,4-position (site **b**) is only destabilized by 0.3 kcal·mol^{-1} with respect to site **a**. Although η^2-coordination of C_6H_5Cl to **3** induces a loss in resonance energy in the aromatic ring,[23] the arene is bound by ∼17 kcal·mol^{-1}. These η^2-C_6H_5Cl adducts are much less stable than the C−Cl OA product but are similar in energy to the C−H OA products. Hence, an equilibrium may exist between the η^2-coordination and C−H OA products. In addition to these π-bound arene adducts, the arene can coordinate via one or more C−X σ bonds making σ-complexes. These complexes are all less stable but are on the reaction path for the C−X OAs.

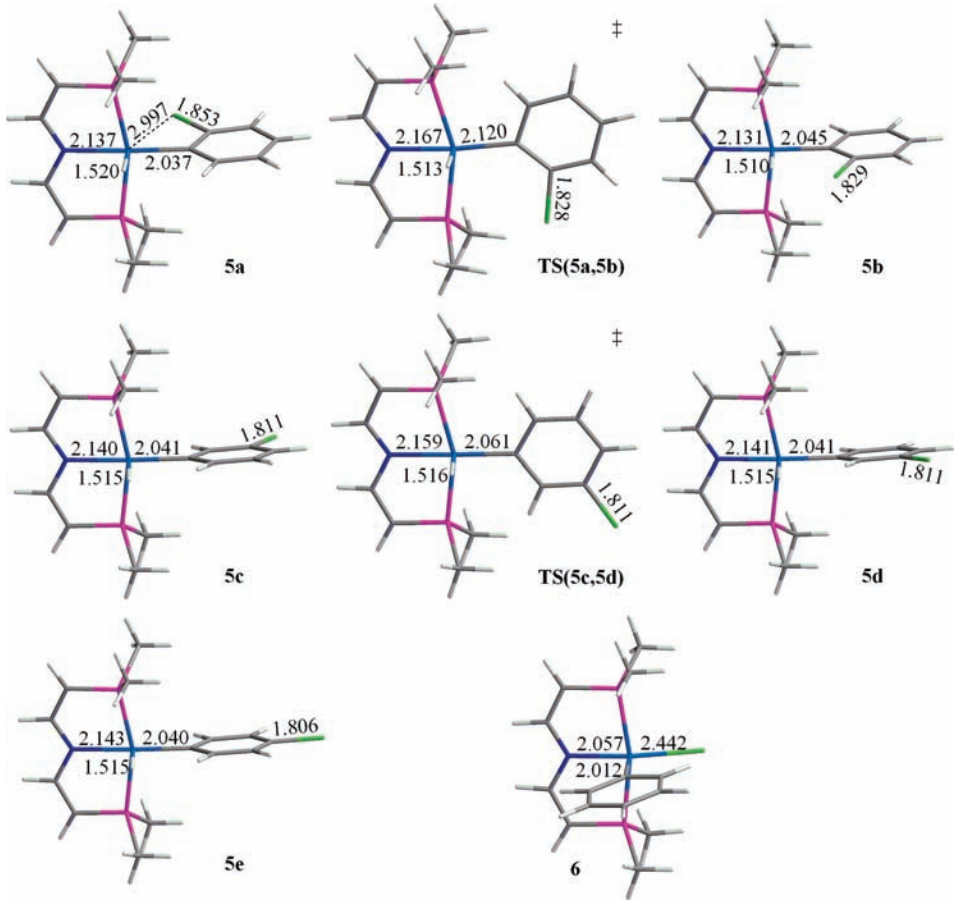

Figure 3. Optimized geometries of **5a**−**5e**, **6**, **TS(5a,5b)**, and **TS(5c,5d)**.

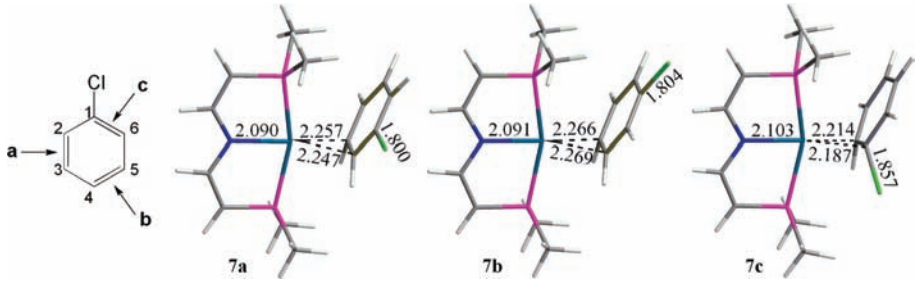

Figure 4. Optimized geometries of isomers of η^2-C_6H_5Cl complex **7.**

C−H σ-Complexes and Transition States for C−H OA. Upon the addition of chlorobenzene **4**, we assume that the key intermediate (PNP)Rh^I **3** undergoes C−H OA reactions via Ir···H−C σ-complex (agostic) intermediates: from **IM2-a** to **5a**, from **IM2-b** to **5b**, from **IM2-c** to **5c**, from **IM2-d** to **5d**, and from **IM2-e** to **5e**. Optimized geometries of σ-complexes, **IM2-a**−**IM2-e** and the corresponding transition states, **TS2-a**−**TS2-e** are shown in Figure 5. The Ir−H and Ir−C bonds have nearly formed in the transition states as indicated by their short distances. Relative to **3** + **4**, the formation of the σ-complexes **IM2-a**−**IM2-e** is exothermic (ΔH = −12.8, −8.7, −9.7, −9.8, −9.9 kcal·mol^{-1}) but endogonic (ΔG = 3.0, 2.8, 2.3, 2.2, 2.0 kcal·mol^{-1}). However, these σ-complexes are less stable than the η^2-C_6H_5Cl π-complexes (i.e., **7a** is 6.9 kcal·mol^{-1} lower in energy than **IM2-a**). When we searched for the C−H OA transition states for the formation of **5a**−**5e** starting with the η^2-C_6H_5Cl complexes (**7a** and **7b**), the same transition states, **TS1-a**−**TS1-e**, were obtained. Hence, we will take the more stable **7a** as the intermediate for the formation of **5a**−**5d** and **7b** as the one used for the formation of **7e**. The five C−H OA reactions, are all exothermic and exergonic. Unlike the previously explored Ir systems, in which C−H OA reactions require relatively low activation barriers (less than 10 kcal·mol^{-1}), the activation barriers ($\Delta G^{\ddagger}$) for the Rh system are somewhat higher ($\Delta G^{\ddagger}$ = 16.7 (**a**), 13.7 (**b**), 11.6 (**c**), 11.4 (**d**), and 11.9 (**e**) kcal·mol^{-1}). These barriers are not negligible and will compete with the barrier of C−Cl OA reaction as we will show.

C−Cl σ-Complexes and Transition States for C−Cl OA. The 14-electron (PNP)Rh^I fragment undergoes C−Cl OA to **6** via σ-complex **IM3** and **TS3**. (Scheme 2) The optimized geometries of **IM3** and **TS3** are shown in Figure 6. The formation of **IM3** is exothermic (−12.0 kcal·mol^{-1}) and slightly exergonic (−0.6 kcal·mol^{-1}). Again, since the η^2-C_6H_5Cl complexes are also the potential intermediates prior to this OA reaction and **7a** is more stable than the **IM3** by 3.3 kcal·mol^{-1}, there is possibility that **6a** is also derived from **7a**, i.e., the less stable **IM3** may not play an important role Hence, we also searched for the C−Cl OA transition states for the formation of **6** starting with the η^2-C_6H_5Cl complex **7a**. Not surprisingly, the same transition state, **TS3**, was obtained. Hence, **7a** is taken as the energetically important intermediate for the formation of **6**. The activation barrier ($\Delta G^{\ddagger}$) of C−Cl OA is 16.0 kcal·mol^{-1}, which is very close to the C−H OA activation barriers. Together with the fact that C−H OA products (**5a**−**5e**) are substantially less stable than and C−Cl OA product (**6**), only C−Cl OA product was observed by the experiment.[12]

The energetic data of entire set of reactions of (PNP)Rh^I(Ph)(Me) (**1**) with chlorobenzene (**4**) are summarized by a ΔG potential energy diagram in Figure 7. All energy are relative to the starting materials. The entire reaction is exergonic by 49.6 kcal·mol^{-1}. The first C−C RE has a 23.3 kcal·mol^{-1}

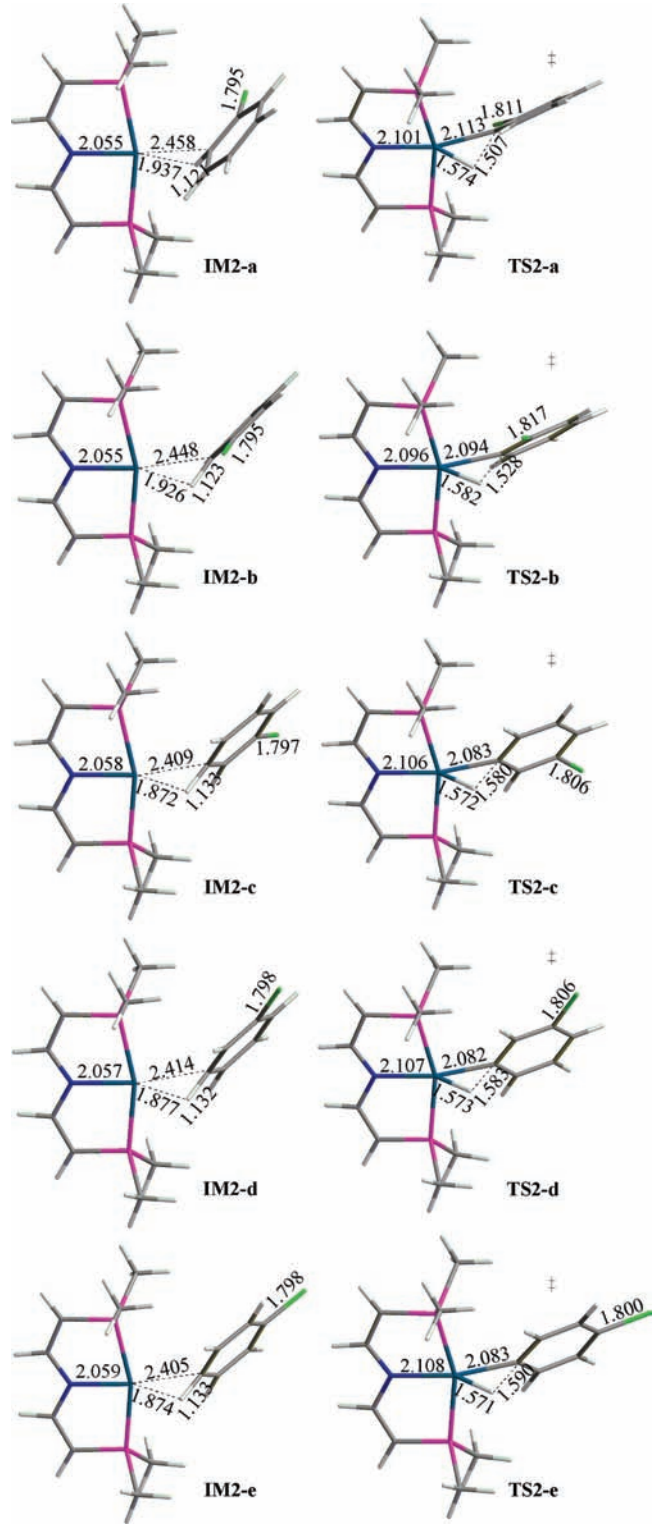

Figure 5. Optimized geometries of **IM2-a**−**IM2-e** and **TS2-a**−**TS2-e**.

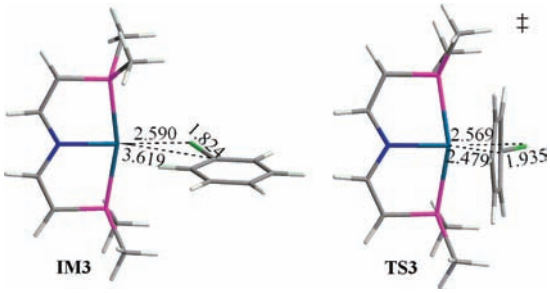

Figure 6. Optimized geometries of **IM3** and **TS3**.

activation (free-energy) barrier, which is higher than those for the following OA reactions; this result is in agreement with the kinetic study, which showed that C−C RE of (PNP)Rh(Ph)(Me) is the rate-determining step. The activation free-energy barrier for the C−Cl OA reaction, **7a** to **TS3**, is only 16.0 kcal·mol^{-1}, which is lower than the barrier for the C−H OA to the most stable C−H OA products, **7a** to **TS2-a** ($\Delta G^{\ddagger} = 16.7$ kcal·mol^{-1}) but slightly higher than the barrier for the C−H OA to the less stable C−H OA product from **7a** to **TS2-b** ($\Delta G^{\ddagger} = 13.6$ kcal·mol^{-1}). Although the barriers for C−H OA are comparable to that for C−Cl OA, the C−Cl OA product (**6**) is thermodynamically much more stable than any of the C−H OA products (**5a**−**5e**). Furthermore, the C−H OA products are energetically unstable; **5a** is only 1 kcal·mol^{-1} lower energy than the intermediate **7a** and all other isomers (**5a**−**5e**) are even less stable than **7a**. Hence, C−H OA products, if any are formed, are too short-lived to be detected by these experiments. Being both thermodynamically favored and kinetically comparable, C−Cl OA ultimately leads to the only observable final product, which is consistent with the experimental observation that the C−Cl OA product was observed exclusively.

Conclusions

A major motivation of this research is to compare the reaction coordinates for C−H oxidative addition (OA) versus C−X OA of haloarenes to late transition metals to address issues of kinetic and thermodynamic selectivity. To this end, OA reactions of chlorobenzene by the netural Rh^{I} complex (PNP)Rh^{I} (**7**) [PNP = bis(*Z*-2 (dimethylphosphino)vinyl)amino] are investigated with density functional theory (DFT). Our calculations show that the PNP-based Rh^{I} system exhibits different activities for aromatic C−H and C−Cl activation when compared to its PNP-based Ir^{I} analogs,[24] which possess controllable selectivities for kinetically preferred aromatic C−H OA and thermodynamically preferred C−Cl OA. For PNP-based Rh^{I} system, since C−Cl OA activation is kinetically competitive and thermodynamically

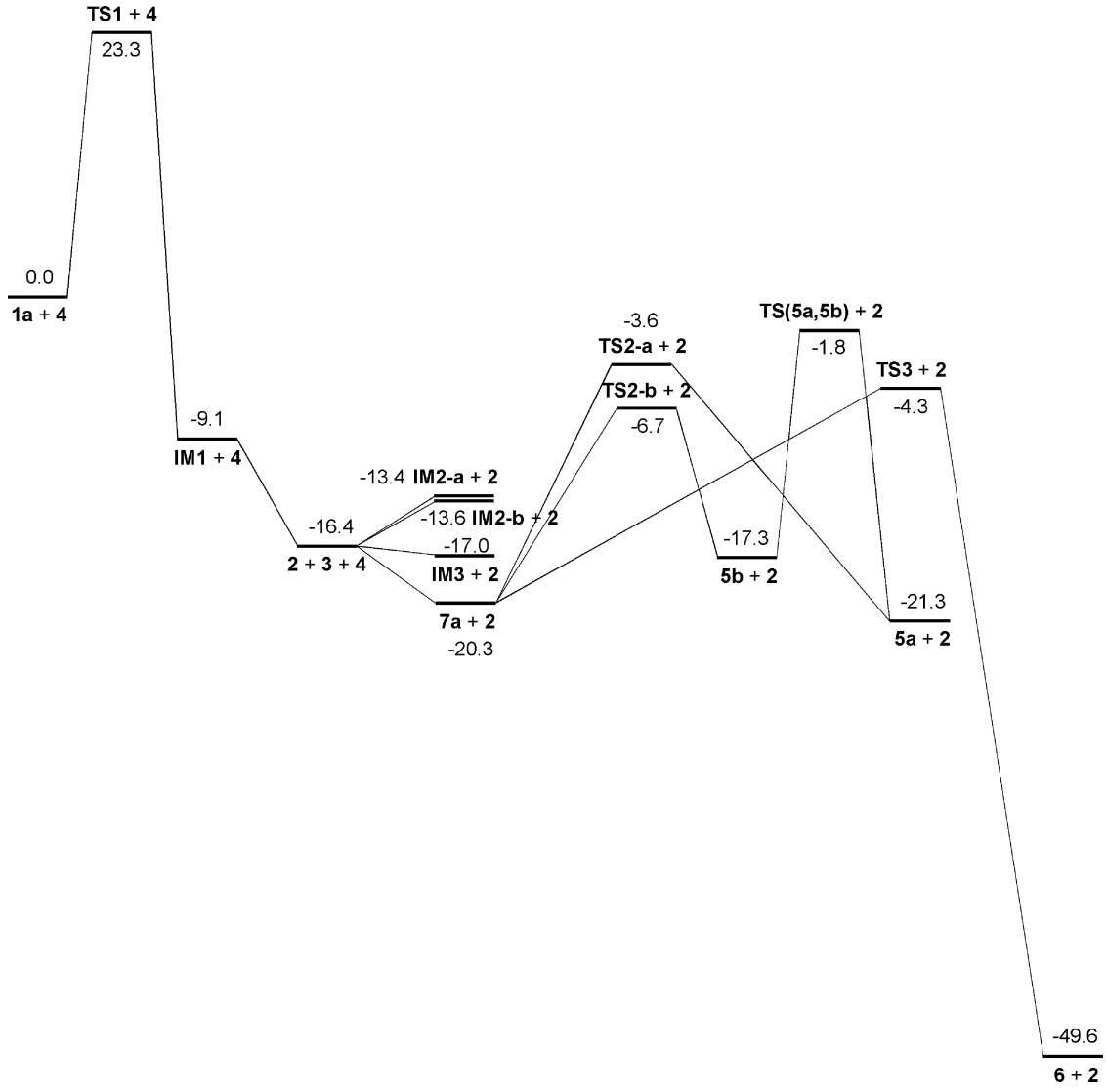

Figure 7. Energy (ΔG) diagram for oxidative additions of (PNP)Rh^{I} with chlorobenzene. The energy numbers are relative to the starting materials.

favorable, only the C−Cl OA product was observed even at room temperature.[25] The C−H OA products are much long-lived for the Ir (5d metal) than for the Rh (4d metal) complexes. For the Ir system, C−Cl OA occurs only at temperatures higher than 100 °C. Therefore, C−H OA in haloarenes is likely to be more successful with Ir than Rh, while C−Cl OA in haloarenes is likely to be more successful with Rh than Ir. We expect that a similar scenarios for 4d versus 5d metals may appear in other transition metal systems that are capable of OA reactions upon the addition of haloarenes.

Acknowledgment. We acknowledge the The Welch Foundation (Grant No. A-0648) for financial support. Dr. Lisa Perez (TAMU) is acknowledged for the PBE0 and M05 calculations.

Supporting Information Available: Tables with total energies and thermochemical data. Energy diagram. This material is available free of charge via the Internet at http://pubs.acs.org.

References and Notes

(1) (a) Arndsten, B. A.; Bergman, R. G.; Mobley, T. A.; Peterson, T. H. *Acc. Chem. Res.* **1995**, *28*, 154. (b) Shilov, A. E.; Shul'pin, G. B. *Chem. Rev.* **1997**, *97*, 2879. (c) Niu, S.; Hall, M. B. *Chem. Rev.* **2000**, *100*, 353. (d) Ritleng, V.; Sirlin, C.; Pfeffer, M. *Chem. Rev.* **2002**, *102*, 1731, and reference cited therein.

(2) Shilov, A. E. *Pure Appl. Chem.* **1978**, *50*, 725.

(3) Janowicz, A. H.; Bergman, R. G. *J. Am. Chem. Soc.* **1982**, *104*, 352.

(4) Jones, W. D.; Feher, F. *Organometallics* **1983**, *2*, 562.

(5) Hoyano, J. K.; McMaster, A. D; Graham, W. A. G. *J. Am. Chem. Soc.* **1983**, *105*, 7190.

(6) (a) Cotton, S. A. *Chemistry of Precious Metals*; Chapman and Hall: London, 1997; p 78. (b) Dickson, R. S. *Organometallic Chemistry of Rodium and Iridium*; Academic Press: New York, 1983.

(7) (a) Niu, S.; Hall, M. B. *J. Am. Chem. Soc.* **1999**, *121*, 3992. (b) Fan, Y.; Cui, X.; Burgess, K.; Hall, M. B. *J. Am. Chem. Soc.* **2004**, *126*, 16688. (c) Zhang, X.; Kanzelberger, M.; Emge, T. J.; Goldman, A. S. *J. Am. Chem. Soc.* **2004**, *126*, 13192. (d) Davies, D. L.; Donald, S. M. A.; Al-Duaij, O.; Macgregor, S. A.; Pölleth, M. *J. Am. Chem. Soc.* **2006**, *128*, 4210.

(8) (a) Crabtree, R. H. *The Organometallic Chemistry of the Transition Metals*, 3rd ed.; Wiley-Interscience: New York, 2001; p 149. (b) Mureinik, R. J.; Weitzberg, M.; Blum, J. *Inorg. Chem.* **1979**, *18*, 915.

(9) Ben-Ari, E.; Gandelman, M; Rozenberg, H.; Shimon, L. J. W.; Milstein, D. *J. Am. Chem. Soc.* **2003**, *125*, 4714.

(10) Hermann, D.; Gandelman, M.; Rozenberg, H.; Shimon, L. J. W.; Milstein, D. *Organometallics* **2002**, *21*, 812.

(11) Fan, L.; Parkin, S.; Ozerov, O. V. *J. Am. Chem. Soc.* **2005**, *127*, 16772.

(12) Gatard, S.; Çelenligil-Çetin, R.; Guo, C.; Foxman, B. M.; Ozerov, O. V. *J. Am. Chem. Soc.* **2006**, *128*, 2808.

(13) Cundari, T. R.; Vaddadi, S. *Inorg. Chim. Acta* **2004**, *357*, 2863.

(14) Frisch, M. J.; Trucks, G. W.; Schlegel, H. B.; Scuseria, G. E.; Robb, M. A.; Cheeseman, J. R.; Montgomery, J. A., Jr.; Vreven, T.; Kudin, K. N.; Burant, J. C.; Millam, J. M.; Iyengar, S. S.; Tomasi, J.; Barone, V.; Mennucci, B.; Cossi, M.; Scalmani, G.; Rega, N.; Petersson, G. A.; Nakatsuji, H.; Hada, M.; Ehara, M.; Toyota, K.; Fukuda, R.; Hasegawa, J.; Ishida, M.; Nakajima, T.; Honda, Y.; Kitao, O.; Nakai, H.; Klene, M.; Li, X.; Knox, J. E.; Hratchian, H. P.; Cross, J. B.; Adamo, C.; Jaramillo, J.; Gomperts, R.; Stratmann, R. E.; Yazyev, O.; Austin, A. J.; Cammi, R.; Pomelli, C.; Ochterski, J. W.; Ayala, P. Y.; Morokuma, K.; Voth, G. A.; Salvador, P.; Dannenberg, J. J.; Zakrzewski, V. G.; Dapprich, S.; Daniels, A. D.; Strain, M. C.; Farkas, O.; Malick, D. K.; Rabuck, A. D.; Raghavachari, K.; Foresman, J. B.; Ortiz, J. V.; Cui, Q.; Baboul, A. G.; Clifford, S.; Cioslowski, J.; Stefanov, B. B.; Liu, G.; Liashenko, A.; Piskorz, P.; Komaromi, I.; Martin, R. L.; Fox, D. J.; Keith, T.; Al-Laham, M. A.; Peng, C. Y.; Nanayakkara, A.; Challacombe, M.; Gill, P. M. W.; Johnson, B.; Chen, W.; Wong, M. W.; Gonzalez, C.; Pople, J. A. *Gaussian 03*, revision B.4; Gaussian, Inc.: Pittsburgh, PA, 2003.

(15) (a) Stephens, P. J.; Devlin, F. J.; Chabalowski, C. F.; Frisch, M. *J. Phys. Chem.* **1994**, *98*, 11623. (b) Becke, A. D. *J. Chem. Phys.* **1993**, *98*, 5648. (c) Lee, C.; Yang, W.; Parr, R. G. *Phys. Rev. B* **1988**, *37*, 785.

(16) Peng, C.; Ayala, P. Y.; Schlegel, H. B.; Frisch, M. J. *J. Comput. Chem.* **1996**, *17*, 49.

(17) Hay, P. J.; Wadt, W. R. *J. Chem. Phys.* **1985**, *82*, 299.

(18) Couty, M.; Hall, M. B. *J. Comput. Chem.* **1996**, *17*, 1359.

(19) Ehlers, A. W.; Böhme, M.; Dapprich, S.; Gobbi, A.; Höllwarth, A.; Jonas, V.; Köhler, K. F.; Stegmann, R.; Veldkamp, A.; Frenking, G. *Chem. Phys. Lett.* **1993**, *208*, 111.

(20) Check, C. E.; Faust, T. O.; Bailey, J. M.; Wright, B. J.; Gilbert, T. M.; Sunderlin, L. S. *J. Phys. Chem. A* **2001**, *105*, 8111.

(21) (a) Petersson, G. A.; Al-Laham, M. A. *J. Chem. Phys.* **1991**, *94*, 6081. (b) Petersson, G. A.; Bennett, A.; Tensfeldt, T. G.; Al-Laham, M. A.; Shirley, W. A.; Mantzaris, J. *J. Chem. Phys.* **1988**, *89*, 2193. (c) Foresman, J. B.; Frisch, Æ.; *Exploring Chemistry with Electronic Structure Methods*, 2nd ed.; Gaussian, Inc.: Pittsburgh, PA, p 110. The 6-31G(d′) basis set has the d polarization functions for C, N, O, and F taken from the 6-311G basis set, instead of the original arbitrarily assigned value of 0.8 used in the 6-31G(d) basis set.

(22) Belt, S. T.; Helliwell, M.; Jones, W. D.; Partridge, M. G.; Perutz, R. N. *J. Am. Chem. Soc.* **1993**, *115*, 1429.

(23) Schilling, B. E. R.; Hoffmann, R.; Lichtenberger, D. L. *J. Am. Chem. Soc.* **1979**, *101*, 585.

(24) Wu, H.; Hall, M. B. *Dalton Trans.* **2009**, 5933.

(25) To examine the robustness of these conclusions, free energies for the key intermediates and transition states were also calculated with the PBE0 (PBE1PBE) [Perdew, J. P.; Ernzerhof, M.; Burke, K. *J. Chem. Phys.* **1997**, *105*, 9982]and the M05[Zhao, Y.; Schultz, N. E.; Truhlar, D. G. *J. Chem. Theory Comput.* **2006**, *2*, 364]functionals. With respect to the haloarene π-complex (**7a**), the reaction free energies to the product for C−H OA (**5a**) are−1.0, +0.5, and +10.5 kcal mol^{-1}, while those to the product for C−Cl OA (**6**) are−29.3,−27.5, and−18.9 kcal·mol^{-1} for B3LYP, PBE0, and M05, respectively. The highest barriers for these two reactions, C−H OA (**TS2-a**) vs C−Cl OA (**TS3**), are predicted to be somewhat similar by all the functionals, $\Delta G^{\ddagger} = 16.7$ vs 16.0 for B3LYP; 16.7 vs 19.2 for PBE0, and 20.2 vs 18.7 kcal·mol^{-1} for M05, respectively. Thus, all functionals agree that if any C−H OA addition products were to form, they would be driven thermodynamically to the C−Cl OA product. Furthermore, M05, the newest and the most highly parameterized of these functionals, predicts an even stronger kinetic preference for the C−Cl OA product than B3LYP although PBE0 predicts a kinetic preference for all the C−H OA products. Complete details are given in the Supporting Information.

JP902826W